

# Parton Percolation in Nuclear Collisions

**Helmut Satz**

Fakultät für Physik, Universität Bielefeld

D-33501 Bielefeld, Germany

and

Departamento de Física, Instituto Superior Técnico

P-1049 001 Lisboa, Portugal

## **Abstract**

An essential prerequisite for quark-gluon plasma production in nuclear collisions is cross-talk between the partons from different nucleons in the colliding nuclei. The initial density of partons is determined by the parton distribution functions obtained from deep inelastic lepton-hadron scattering and by the nuclear geometry; it increases with increasing  $A$  and/or  $\sqrt{s}$ . In the transverse collision plane, this results in clusters of overlapping partons, and at some critical density, the cluster size suddenly reaches the size of the system. The onset of large-scale cross-talk through color connection thus occurs as geometric critical behavior. Percolation theory specifies the details of this transition, which leads to the formation of a condensate of deconfined partons. Given sufficient time, this condensate could eventually thermalize. However, already the onset of parton condensation in the initial state, without subsequent thermalization, leads to a number of interesting observable consequences.

# 1 Initial State Conditions

Statistical QCD predicts that with increasing temperature, strongly interacting matter will undergo a transition from a hadronic phase to a plasma of deconfined quarks and gluons. In the hadronic state, the chiral symmetry of the QCD Lagrangian (for massless quarks) is spontaneously broken; in the quark-gluon plasma, it is restored. These predictions are the result of finite temperature lattice QCD studies, and for the calculations it is crucial that they deal with a thermal medium, i.e., with equilibrium thermodynamics.

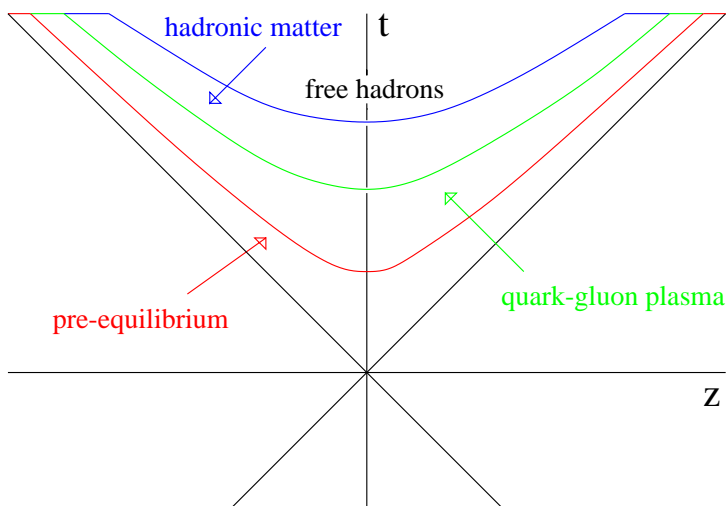


Figure 1: The expected evolution of a nuclear collision

The initial state of two colliding nuclei is clearly a non-equilibrium configuration. The canonical view of its evolution is schematically illustrated in Fig. 1. After the collision, there is a short pre-equilibrium stage, in which the primary partons of the colliding nuclei interact, multiply and then thermalize to form a quark-gluon plasma. This QGP then expands, cools and hadronizes. A prerequisite for the equilibration process is evidently that the partons originating from different nucleons form a large-scale interconnected system. If there is no “cross talk” between partons from different nucleons, thermalization is not possible. The problem of color connection has been studied in hadron production through  $W^+W^-$  decay at LEP. The  $W$ 's are produced essentially at rest in the annihilation of an energetic  $e^+e^-$  pair (see Fig. 2), and it is possible to compare the reaction in which both  $W$ 's produce hadronic jets to that in which one decays leptonically. If there is cross talk between the decay quarks of one  $W$  with those from the other, the multiplicity of the four-jet decay is predicted to be less than twice that in the two-jet decay [1]. The data show no such reduction, suggesting that the decay quarks from different  $W$ 's don't communicate [2].

It is therefore necessary to determine under what conditions the initial state parton configurations can lead to color connection, and more specifically, if variations of the initial state can lead to a transition from disconnected to connected partonic clusters. The results of such a study of the pre-equilibrium state in nuclear collisions do not depend on the subsequent evolution and thus in particular not require any kind of thermalization.

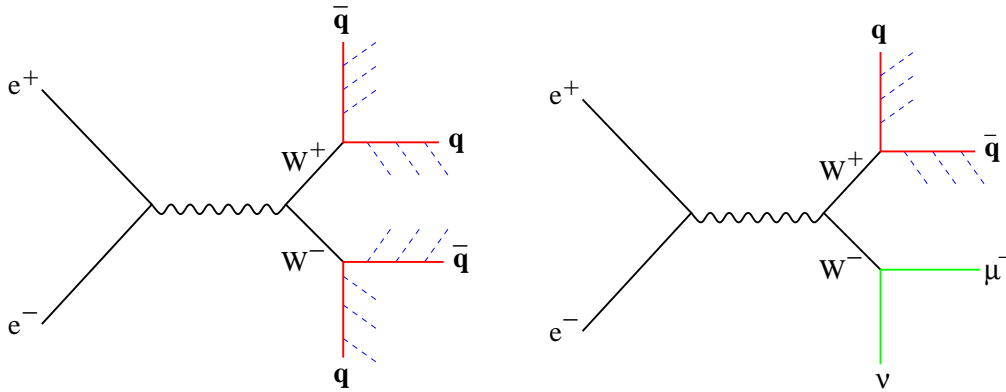


Figure 2: Four-jet and two-jet decays of  $W^+W^-$  pairs in  $e^+e^-$  annihilation at LEP.

The structural problem underlying the transition from disconnected to connected systems of many components is a very general one, ranging from clustering in spin systems to the formation of galaxies. The formalism is given by percolation theory, which describes geometric critical behavior [3]. We shall return to the basic idea a little later on.

## 2 Partons in Nuclei

If you look at a fast nucleon coming at you, what do you see? The answer depends on who's looking. Another nucleon or a pion sees a disc of radius  $r \simeq 1$  fm and a certain greyness. A hard photon, with a resolution scale  $Q^{-1} \ll 1$  fm, sees a swarm of partons. How many there are depends on the resolution scale: given a finer scale, you can see smaller partons, and there are more the harder you look (Fig. 3). The partons in a nucleon have a transverse size  $r_T$  determined by their intrinsic transverse momentum  $k_T$ , with  $r_T \simeq 1/k_T$ . The scale  $Q^{-1}$  specifies the minimum  $k_T^{-1}$  resolved, so the probing photon sees all partons in the range  $0 \leq k_T \leq Q$ .

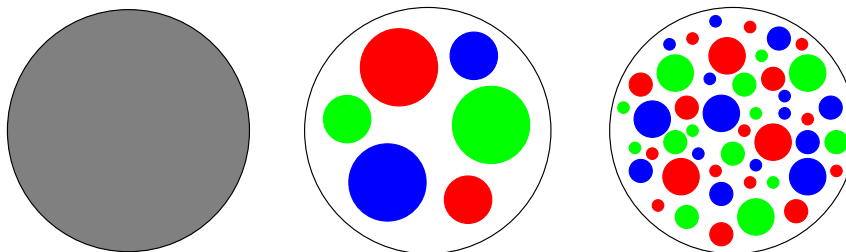


Figure 3: The structure of an incoming nucleon seen (left to right) for increasing resolution

The momentum  $p$  of the incoming nucleon is distributed among the partons; a parton of momentum  $k$  carries the fraction  $x = k/p$ . In deep inelastic scattering experiments, the distribution of partons in a nucleon is determined for given  $x$  and  $Q$ . Denoting the gluon

content by  $g(x, Q)$ , that of quarks and antiquarks by  $q(x, Q)$  and  $\bar{q}(x, Q)$ , respectively, we have the overall momentum conservation sum rule

$$\int_0^1 dx x \{g(x, Q) + \sum_i [q_i(x, Q) + \bar{q}_i(x, Q)]\} = 1, \quad (1)$$

where  $i$  counts the number of quark flavors.

The number of partons in a nucleon at rapidity  $y$ , as seen by a photon of scale  $Q$ , is thus given by

$$\frac{dN}{dy} = x \{g(x, Q) + \sum_i [q_i(x, Q) + \bar{q}_i(x, Q)]\}, \quad (2)$$

where  $x = (k_0 + k_L)/(p_0 + p_L)$  in terms of the parton and nucleon energies  $k_0$ ,  $p_0$  and longitudinal momenta  $k_L$ ,  $p_L$ . Since the scale  $Q$  specifies the maximum  $k_T$  resolved,  $dN/dy$  in Eq. (2) gives us the total number of partons in the range  $0 \leq k_T \leq Q$ .

In a minimum bias nucleon-nucleon collision, the transverse parton size itself determines the resolution: it sets the scale at which partons ‘probe each other’ in the colliding nucleons, so that here the highest relevant  $k_T$  fixes  $Q$ . Since at  $y = 0$ , the fractional momentum is  $x = k_T/\sqrt{s}$ , Eq. (2) provides at given  $\sqrt{s}$  the total number of partons of transverse momenta up to  $Q$ .

As mentioned, the quark and gluon distributions in a nucleon are determined from deep inelastic scattering data. In Fig. 4, we show the resulting variation of  $(dN/dy)_{y=0}$  as function of  $Q^2 \simeq \langle k_T^2 \rangle$  for two values of the c.m.s. energy,  $\sqrt{s} = 20$  GeV (SPS) and 200 GeV (RHIC), using the GRV94DIS parametrization [4], which is particularly suitable for our kinematic range. It is evident that with increasing  $Q^2$ , more and more partons of decreasing size come into play, so that  $(dN/dy)_{y=0}$  increases strongly with  $Q$ . It is also clear that at higher collision energy, there are more partons – at RHIC two times more than at SPS. The slow decrease at large  $Q^2$  is due to kinematic constraints: at fixed  $\sqrt{s}$ , increasing  $Q^2$  means increasing  $x$  and hence decreasing gluon or sea quark density.

## 3 Partons in Nuclear Collisions

Consider now the collision of two heavy nuclei at high energy, as seen in the overall center of mass. The Lorentz-contraction in the longitudinal direction makes it a collision of two thin discs, so that in the transverse plane, the parton density increases with  $A$ . The partons from different nucleon begin to overlap and form clusters: see Fig. 5. How does the cluster size grow with parton density, and when does it reach the dimension of the total transverse collision area? These are precisely the questions addressed by percolation theory, so that here we make a small interlude.

### 3.1 Percolation Theory

Consider placing  $N$  small circular discs (‘partons’) of radius  $r$  onto a large circular manifold (‘the transverse nuclear plane’) of radius  $R \gg r$ ; the small discs may overlap. With increasing parton density  $n \equiv N/\pi R^2$ , this overlap will lead to more and larger connected

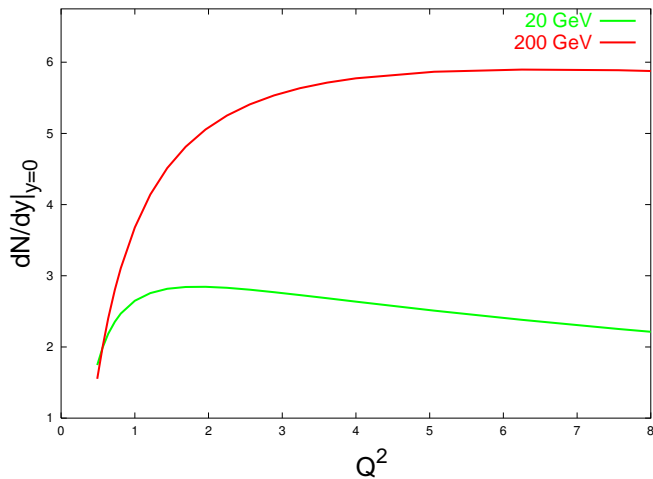


Figure 4: Parton density at central rapidity as function of the resolution scale  $Q$  at  $\sqrt{s} = 20$  and 200 GeV, using PDF GRV94DIS.

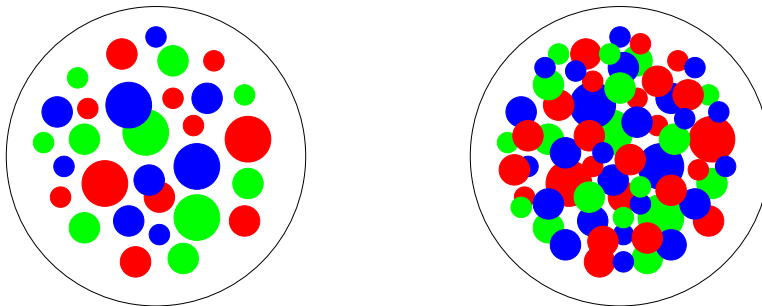


Figure 5: Partonic cluster structure in the transverse collision plane at low (left) and high (right) parton density

partonic clusters. The striking feature of this phenomenon is that the average cluster size  $S_{cl}$  does not grow as some power of  $n$ ; instead, it increases very suddenly from very small to very large values (see Fig. 6). This suggests some kind of geometric critical behavior, and in fact in the ‘thermodynamic limit’  $N \rightarrow \infty$ ,  $R \rightarrow \infty$ , the cluster size diverges at a critical threshold value  $n_c$  of the density  $n$ ,

$$S_{cl} \sim (n_c - n)^{-\gamma}, \quad (3)$$

as  $n \rightarrow n_c$  from below. This appearance of infinite clusters at  $n = n_c$  is defined as percolation: the size of the cluster reaches the size of the system. The divergence is governed by the critical exponent  $\gamma = 43/18$ , determined analytically, while the threshold

$$n_c = \frac{1.128}{\pi r^2} \quad (4)$$

is obtained numerically or through analytical approximation [5]. Hence we obtain in the limit of large systems

$$\frac{N}{\pi R^2} = \frac{1.128}{\pi r^2} \quad (5)$$

as percolation condition. Note that because of parton overlap, the manifold is at percolation not totally covered by discs, even though the overall disc area slightly exceeds that of the manifold:  $N \pi r^2 = 1.128 \pi R^2$ . In fact, one can show that at  $n = n_c$ , the fraction

$$1 - \exp\{-1.128\} \simeq 0.68 \quad (6)$$

of the area  $\pi R^2$  is covered by partonic discs.

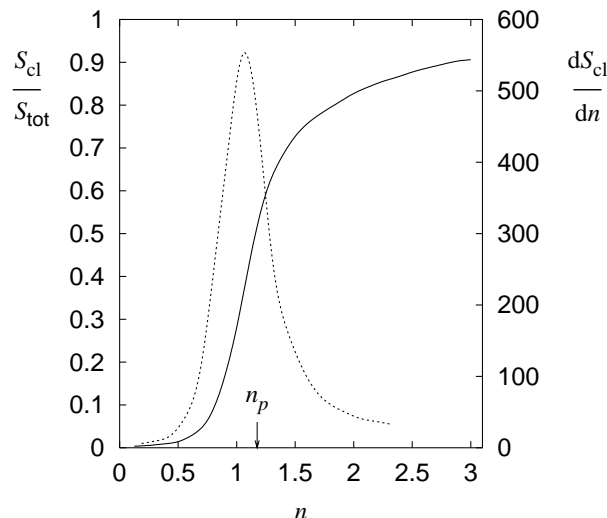


Figure 6: The fractional cluster size and its derivative as function of the parton density  $n$

Before we return to the study of nuclear collisions, we want to comment briefly on the relation between percolation and thermal phase transitions [3, 6]. Some thermal critical behavior, such as the magnetization transition for ferromagnetic spin systems, can be equivalently formulated as percolation. However, percolation seems to be a more general phenomenon and in particular can occur even when the partition function is analytic, i.e., when there is no thermal critical behavior. A specific example of this is the Ising model in a non-vanishing external field, which has a percolation transition even though there is no magnetization transition.

### 3.2 Parton Percolation

The results of the previous subsection tell us that in nuclear collisions there is indeed, as function of parton density, a sudden onset of large-scale color connection. There is a critical density at which the partons form one large cluster, losing their independent existence and their relation to the parent nucleons. Parton percolation [7, 8] is thus the onset of color deconfinement and although it is a necessary prerequisite for any subsequent QGP formation, it does not require or imply any kind of parton thermalization.

To obtain quantitative predictions, we have to specify the relevant scales. The partonic size is through the uncertainty relation determined by its average transverse momentum,

$$\pi r^2 \simeq \frac{\pi}{\langle k_T^2 \rangle}, \quad (7)$$

and as mentioned, for a given resolution scale,  $\langle k_T^2 \rangle \simeq Q^2$ . Given the parton density in a nucleon, we now have to specify the density in a nucleus-nucleus collision. At SPS energy ( $\sqrt{s} \simeq 20$  GeV), the wounded nucleon model appears to work quite well, so that we have in a central  $A - A$  collision

$$\left(\frac{dN}{dy}\right)_{y=0}^{AA} \simeq 2 A \left(\frac{dN}{dy}\right)_{y=0}. \quad (8)$$

It is clear, however, that at higher energies, collision dependent contributions will come into play [9].

For central  $A - A$  collisions, we thus obtain the percolation condition

$$\frac{2A}{\pi A^{2/3}} \left(\frac{dN}{dy}\right)_{y=0} = \frac{1.128}{\pi Q^{-2}} \quad (9)$$

in terms of  $A$ , the resolution scale  $Q$  and the nucleonic parton density obtained in deep inelastic scattering. Let us separate the basic parton contributions from the nuclear dependence and rewrite eq. (9) as

$$\frac{1}{Q^2} \left(\frac{dN}{dy}\right)_{y=0} = \frac{1.128}{2A^{1/3}}. \quad (10)$$

When the l.h.s. of this equation, determined by P.D.F.'s, becomes equal to the r.h.s., fixed by nuclear size, we have the onset of percolation. In Fig. 7, the results are shown for typical SPS and RHIC energies. We thus find that for  $\sqrt{s} = 20$  GeV, there is percolation for  $A \gtrsim 60$ , while for ( $\sqrt{s} = 200$  GeV) it sets in somewhat earlier, for  $A \gtrsim 40$ .

In the case of non-central  $A - A$  collisions, the manifold disc size  $\pi R^2$  has to be replaced by the actual transverse overlap area at the given impact parameter. This overlap area can be determined in a Glauber study, using Woods-Saxon nuclear profiles [10], and the resulting counterpart of eq. (10) then leads to Figs. 8. Here the number  $N_{\text{part}}$  of wounded or participant nucleons is used to specify the centrality of the collision, since this quantity is directly measurable. For  $Pb - Pb$  collisions at  $\sqrt{s} = 20$  GeV, this leads to an onset of percolation at  $N_{\text{part}} \simeq 150$  (corresponding to an impact parameter  $b \simeq 6$  fm), while for  $Au - Au$  at  $\sqrt{s} = 200$  GeV,  $N_{\text{part}} \simeq 80$  (with  $b \simeq 10$  fm) is the threshold.

Beyond the percolation point, we then have a parton condensate, containing interacting and hence color-connected partons of all scales  $k_T \leq Q$ . The percolation point thus specifies the onset of color deconfinement; it says nothing about any subsequent thermalization. If there is eventual thermalization, the partonic momentum  $k_T$  will be related to the temperature  $T$ ; hence the resolution scale  $Q$ , which determines the range of  $k_T$ , is in some sense a precursor of  $T$ . It is thus of interest to check how the percolation value  $Q_s$  is related to the effective nuclear size and to  $\sqrt{s}$ . This is illustrated in Fig. 9 for the

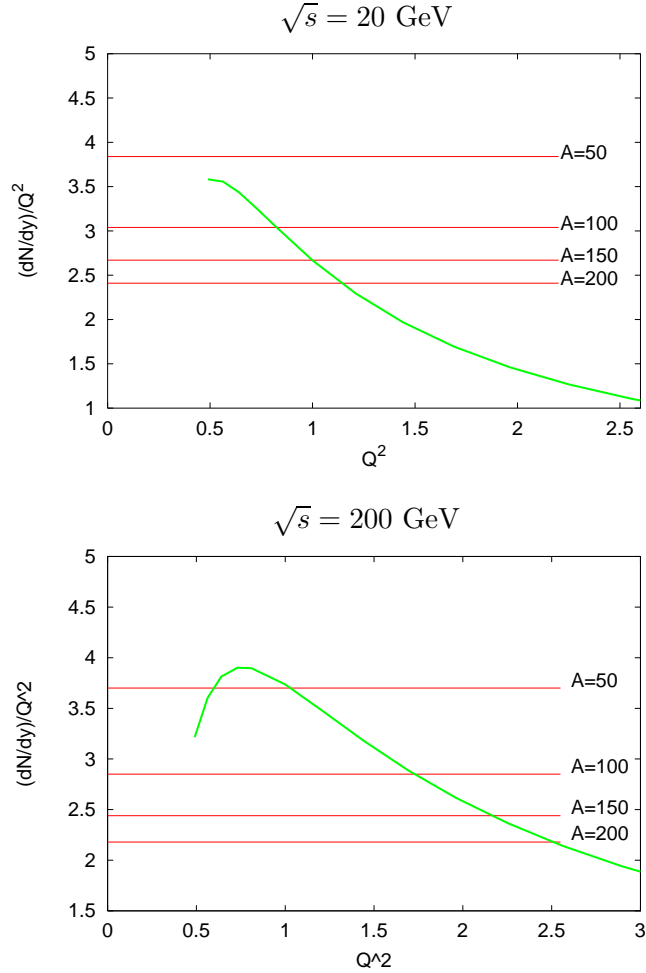


Figure 7: Percolation values of  $Q^2$  for different  $A$  and collision energies.

$A$ -dependence at two energies studied here. In the same figure, we also show the corresponding results as function of centrality at  $A = 200$ . It is seen that bigger  $\sqrt{s}$ , larger  $A$  or more central collisions lead to a ‘hotter’ parton condensate, in the mentioned pre-thermal sense.

## 4 Observable Consequences

We have seen that in nuclear collisions, the parton structure of nucleons leads to critical behavior in the form of parton percolation in the transverse collision plane. This critical behavior is independent of any subsequent thermalization; it is determined by the initial collision conditions in the pre-equilibrium stage.

The parton condensate which is formed through percolation is closely related to the color glass condensate [11] studied for nuclear collisions in the limit of large  $A$  and/or  $\sqrt{s}$ ; the different approaches simply focus on different aspects. In percolation studies, the central topic is the onset of parton condensation in terms of geometric critical behavior. In contrast, the color glass condensate describes the features of the high density limit for



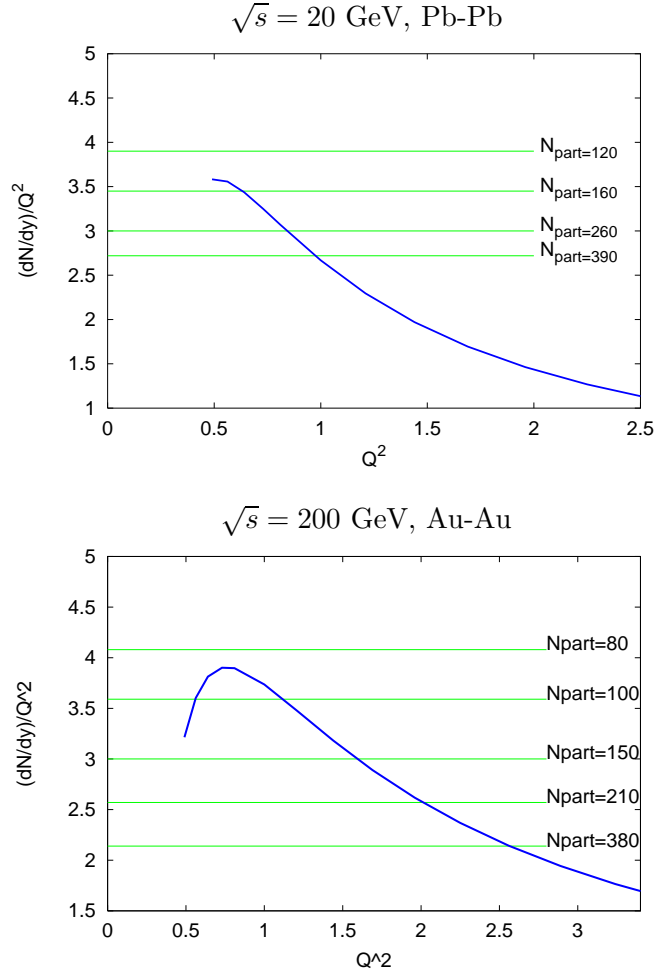


Figure 8: Percolation values of  $Q^2$  for different centralities and collision energies.

the pre-equilibrium partonic medium, in particular in terms of classical fields.

The occurrence of geometric critical behavior in the pre-equilibrium stage of nuclear collisions can lead to observable consequences even if there never is any subsequent thermalization. We note here three possible effects of this kind: charmonium suppression, strangeness enhancement, and energy-independent hadronic source radii.

#### 4.1 Charmonium Suppression

Charmonium states are formed very early in nuclear collisions, with a typical  $J/\psi$  formation time of some 0.2 - 0.3, fm obtained from binding energy or radius. This is also the time needed for the formation of the parton condensate, as determined by  $Q_s^{-1}$ . The  $J/\psi$  thus finds itself in the non-equilibrium medium provided by the parton condensate. The typical scale of the charmonium state thus has to be compared to the intrinsic scale  $Q_s$  of the parton condensate. If the latter is indeed the precursor of temperature, it is also a precursor form of the screening mass. We will therefore assume a charmonium state  $i$  of radius  $r_i$  to be dissociated when  $Q_s > r_i$ . With

$$r_{J/\psi} \simeq (0.9 \text{ GeV})^{-1}, r_\chi \simeq (0.6 \text{ GeV})^{-1} r_{\psi'} \simeq (0.45 \text{ GeV})^{-1}, \quad (11)$$

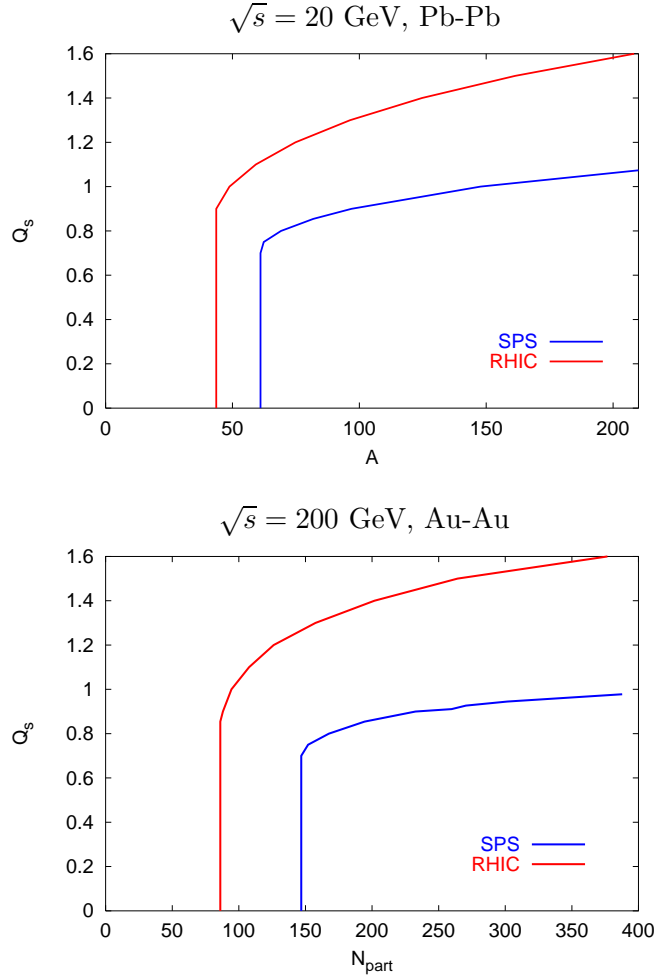


Figure 9: Percolation scale  $Q_s$  vs.  $A$  for  $\sqrt{s} = 20$  and  $200 \text{ GeV}$ .

for the different subthreshold charmonium states, we then obtain the suppression values of  $Q_s$  shown in Fig. 10.

To see what these different suppression points imply for  $J/\psi$  production in nuclear collisions, we recall that in nucleon-nucleon collisions,  $J/\psi$ 's are produced in part through feed-down. Only about 60% of the observed  $J/\psi$ 's are directly produced  $1S$  states; of the remainder, about 30% come from  $\chi_c$  and about 10% from  $\psi'$  decay. Since these decays occur very late in the collision evolution, the parton condensate ‘sees’ and hence suppresses the different charmonium states in the given fractions. From Fig. 10 we thus expect that the survival probability of  $J/\psi$  s in  $Pb-Pb$  collisions at the SPS will show a first anomalous suppression step at about  $N_{\text{part}} \simeq 150$ , since at this point the production fraction from  $\chi_c$  and  $\psi'$  decays is removed. A second drop would be expected around  $N_{\text{part}} \simeq 250$ , since now the directly produced  $J/\psi$ 's are dissociated.

The crucial consequence is the predicted two-step suppression pattern; to obtain reliable numerical values clearly requires the inclusion of more details. In particular, the nuclear geometry, resulting in percolating and non-percolating (‘hot’ vs. ‘cold’) regions in the transverse plane, has to be taken into account correctly in its effect on the suppression. A two-step suppression pattern was first obtained for  $J/\psi$  production in a quark-gluon

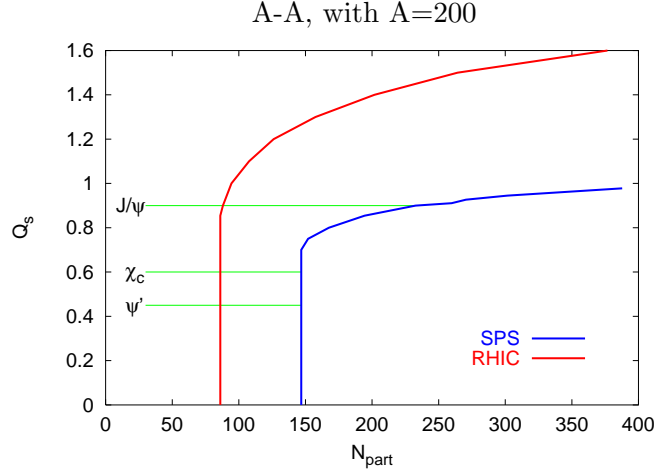


Figure 10: Charmonium dissociation as function of centrality

plasma, since the different charmonium radii lead to dissociation for different screening radii. It now appears that in fact already pre-equilibrium parton condensation leads to a similar result, so that such a pattern, if observed, implies deconfinement but not the formation of a thermalized quark-gluon plasma.

In this connection we note also that the onset points for charmonium dissociation through parton condensation agree fairly well with the ‘steps’ seen in the measured  $J/\psi$  survival probability (see Fig. 11). In view of the mentioned theoretical uncertainties and also because of possible kinematic suppression effects for very central collisions [13], this agreement should so far be considered in a more qualitative way. However, the observed threshold value for the onset of anomalous suppression measured in terms of the energy density is by more than a factor two above the energy density at deconfinement. This seems to support pre-equilibrium deconfinement through parton condensation as underlying mechanism.

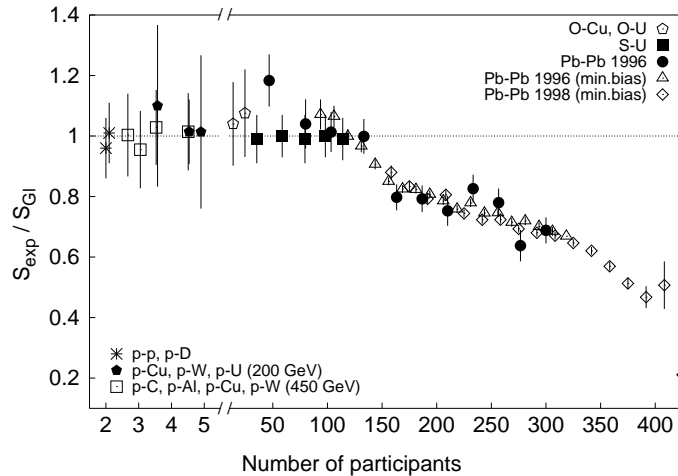


Figure 11: The measured  $J/\psi$  survival probability as function of centrality [12]

## 4.2 Strangeness Enhancement

The relative abundance of the hadrons produced in high energy collisions, from nucleon-nucleon to heavy ion interactions, is well accounted for by an ideal gas of hadronic resonances [14]. The temperature of this gas converges at high energies to  $T_H \simeq 150 - 180$  MeV, i.e., to the confinement temperature obtained in lattice QCD for low baryon density (see Fig. 12 for a compilation from nucleus-nucleus collisions [15]). The baryochemical potential depends on the baryon number content of the initial state, decreasing from values around  $\mu_B \simeq 0.5$  GeV in heavy ion collisions at the AGS to near zero for  $p - p/p - \bar{p}$  and RHIC heavy ion data.

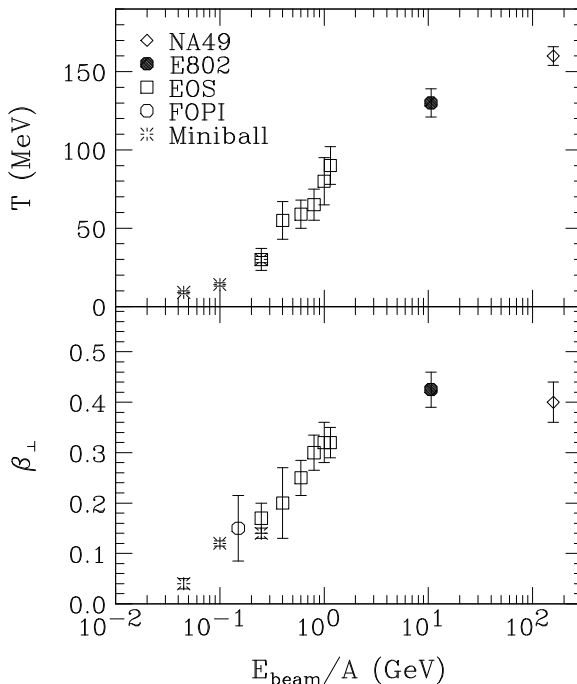


Figure 12: The freeze-out temperature obtained from hadron resonance abundances in nuclear collisions at different energies (top), and the transverse expansion velocity obtained from the corresponding hadronic  $p_T$  spectra (bottom), compiled in [15].

The only ‘flaw’ in this picture is that in the elementary  $p - p/p - \bar{p}$  collisions one observes reduced strangeness production: the relative abundance of strange hadrons is reduced by a factor dependent only on its content of strange quarks/antiquarks. This strangeness suppression disappears for high energy heavy ion collisions.

The dependence of strangeness abundance on the density of interacting hadrons can be accounted for if strangeness conservation is assumed to hold locally [16]. In a thermal medium of temperature  $T$  and overall volume  $V$ , the relative phase space weight (Boltzmann factor) for the presence of a strange particle of mass  $m$  is given by  $\exp\{-m/T\}$ . If, however, the medium contains only one such strange particle, and if strangeness conservation is taken to hold locally within some correlation volume  $V_0 \ll V$ , then the correct Boltzmann factor should be  $\exp\{-2m/T\}$ , since the simultaneous presence of the strange particle and its antiparticle requires the expenditure of energy  $2m$ . The crucial point here

is the assumed local nature of strangeness conservation: the factor  $\exp\{-m/T\}$  would be correct if the single strange particle could be compensated by a ‘far away’ antiparticle somewhere else in the overall volume  $V$ . It is only the requirement of zero strangeness within  $V_0$  that leads to the enhanced suppression. Since a given strange particle and its antiparticle in a really *ideal* gas will eventually separate beyond  $V_0$ , the requirement of local strangeness conservation apparently implies the introduction of a dynamical (i.e., non-ideal) correlation.

To illustrate the effect of this phenomenon, we consider the abundance of kaons in a hadron gas. Given the ideal gas density of kaons,  $n_K(T) = m_K^2 K_2(m_K/T)$ , local strangeness conservation leads to the suppressed form

$$n_K(T, x) = n_K(T) \left\{ \frac{I_1(x)}{I_0(x)} \right\}, \quad (12)$$

where  $x = V_0 n_K(T)$  specifies the number of kaons inside the correlation volume  $V_0$ ;  $I_0$ ,  $I_1$  and  $K_2$  are the corresponding Bessel and Hankel functions of imaginary argument. In the limit of high density or large correlation volume,  $x \rightarrow \infty$ ,  $I_1(x)/I_0(x) \rightarrow 1$ , and the ideal gas abundances are correct. For low density or small correlation volume, i.e., for  $x \rightarrow 0$ ,  $I_1(x)/I_0(x) \ll 1$ , thus resulting in an effective strangeness suppression as compared to the ideal gas abundance of kaons (see Fig. 13).

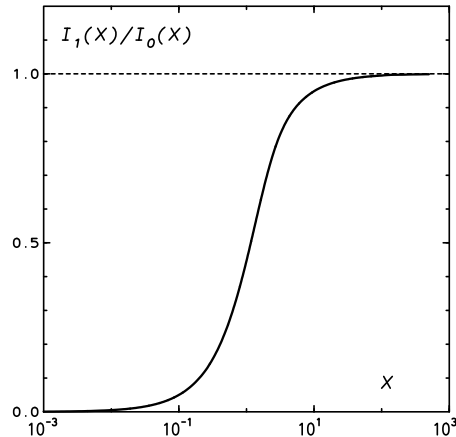


Figure 13: The transition from local to global strangeness conservation

We are thus confronted with the puzzling question of how the transition from suppressed to normal strangeness production occurs. What specifies the correlation volume  $V_0$ ? A rather natural solution to this puzzle is that the abundance of strange hadrons is already determined by the initial state partonic cluster size in the transverse plane: the extension of this cluster specifies  $V_0$ . This means that parton percolation and the corresponding sudden increase of  $V_0$  result in  $I_1/I_0 \rightarrow 1$  and thus trigger the transition to genuine ideal gas abundances of strange particles. More detailed work on this is in progress; an interesting aspect is obviously the resulting correspondence between charmonium suppression and strangeness enhancement.

### 4.3 Thermal or Statistical?

This point is undoubtedly the most speculative of the present considerations. At various stages of the high energy heavy ion program, it has been asked whether a single collision event already produces a thermal medium (‘matter’), or whether each individual event is something like one member of a Gibbs ensemble in thermodynamics, so that only an average over many events results in a thermal pattern.

If we take the extreme point of view that the observable phenomena are determined fully determined by the initial state parton configuration of the colliding nuclei, without any subsequent thermalization, then a single collision does not lead to a thermodynamic medium. Everything is specified by the given nuclear collision configuration, and there will in particular not be any kind of ‘expanding and cooling matter’. This suggests that the source size as determined by HBT interferometry should essentially measure the initial nuclear collision configuration; it should show no dependence on the collision energy and not lead to any ‘medium life-time’, with always  $R_{\text{out}} \simeq R_{\text{side}}$ . Moreover, the transverse expansion velocity should also become constant with increasing collision energy. These features are indeed observed, as shown in Figs. 12 and 14, contrary to all earlier predictions.

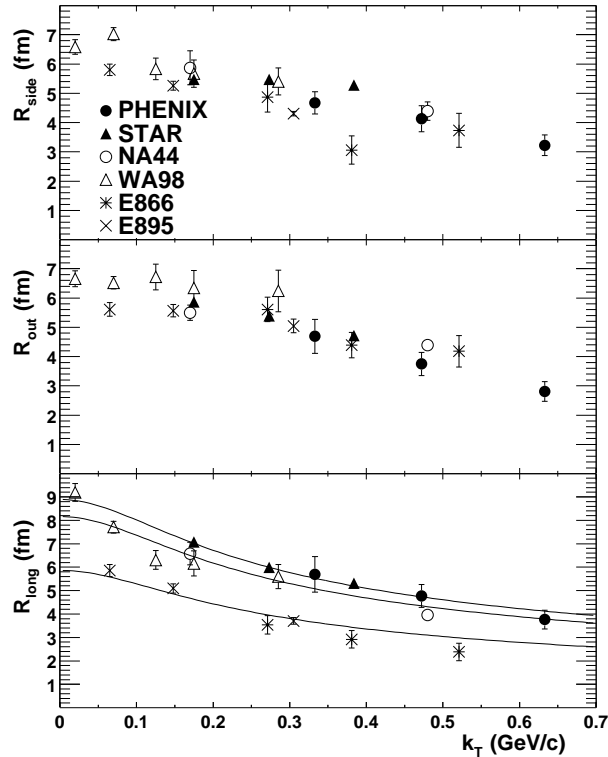


Figure 14: Source radii obtained from HBT interferometry in nuclear collisions at different energies [17].

Perhaps there exist models which nevertheless can reproduce the entire set of present observations in thermal terms. However, it does seem worthwhile to pursue further the possibility that initial state conditions alone already determine them rather naturally,

and to search for some crucial additional observable which would unambiguously indicate event-by-event thermalization.

## Acknowledgements

It is a pleasure to thank S. Digal, S. Fortunato, F. Karsch, C. Lourenço, M. Nardi, P. Petreczky and K. Redlich for many stimulating discussions and helpful comments.

## References

- [1] J. R. Ellis and K. Geiger, *Phys. Lett.* B404 (1997) 230.
- [2] For a recent survey, see P. Abreu, hep-ph/0111395.
- [3] D. Stauffer and A. Aharony, *Introduction to Percolation Theory*, Taylor and Francis, London 1994.
- [4] M. Glück, E. Reya and A. Vogt, *Z. Phys. C* 67 (1995) 433;  
*Eur. Phys. J.C* 5 (1998) 461.
- [5] See e. g., M. S. Isichenko, *Rev. Mod. Phys.* 64 (1992) 961.
- [6] H. Satz, *Comput. Phys. Commun.* 147 (2002) 46.
- [7] M. Nardi and H. Satz, *Phys. Lett. B* 442 (1998) 14;  
H. Satz, *Nucl. Phys. A* 661 (1999) 104c.
- [8] S. Digal et al., *Phys. Lett. B* 549 (2002) 101.
- [9] D. Kharzeev and M. Nardi, *Phys. Lett. B* 507 (2001) 121.
- [10] D. Kharzeev et al., *Z. Phys. C* 74 (1997) 307
- [11] L. McLerran and R. Venugopalan, *Phys. Rev. D* 49 (1994) 2233 and 3352;  
L. McLerran, *Lect. Notes Phys.* 583 (2002) 291.
- [12] M. C. Abreu et al. (NA50), *Phys. Lett. B* 477 (2000) 28 and *Phys. Lett.* 521 (2001) 195
- [13] J.-P. Blaizot, M. Dinh and J.-Y. Ollitrault, *Phys. Rev. Lett.* 85 (2000) 4012.
- [14] F. Becattini et al., *Phys. Rev. C* 64 (2001) 024901.
- [15] Compilation by P. Danielewicz, *Nucl. Phys. A* 685 (2001) 368.
- [16] R. Hagedorn and K. Redlich, *Z. Phys. C* 27 (1985) 541;  
J. Cleymans et al., *Phys. Rev. C* 59 (1999) 1669.
- [17] Compiled in K. Adcox et al. (PHENIX), *Phys. Rev. Lett.* 88 (2002) 192302.